

Sven Ingebrandt · Chi-Kong Yeung · Michael Krause  
Andreas Offenhäusser

## Neuron–transistor coupling: interpretation of individual extracellular recorded signals

Published online: 1 October 2004  
© EBSA 2004

**Abstract** The electrical coupling of randomly migrating neurons from rat explant brain-stem slice cultures to the gates of non-metallized field-effect transistors (FETs) has been investigated. The objective of our work is the precise interpretation of extracellular recorded signal shapes in comparison to the usual patch-clamp protocols to evaluate the possible use of the extracellular recording technique in electrophysiology. The neurons from our explant cultures exhibited strong voltage-gated potassium currents through the plasma membrane. With an improved noise level of the FET set-up, it was possible to record individual extracellular responses without any signal averaging. Cells were attached by patch-clamp pipettes in voltage-clamp mode and stimulated by voltage step pulses. The point contact model, which is the basic model used to describe electrical contact between cell and transistor, has been implemented in the electrical simulation program PSpice. Voltage and current recordings and compensation values from the patch-clamp measurement have been used as input data for the simulation circuit. Extracellular responses were

identified as composed of capacitive current and active potassium current inputs into the adhesion region between the cell and transistor gate. We evaluated the extracellular signal shapes by comparing the capacitive and the slower potassium signal amplitudes. Differences in amplitudes were found, which were interpreted in previous work as enhanced conductance of the attached membrane compared to the average value of the cellular membrane. Our results suggest rather that additional effects like electrodiffusion, ion sensitivity of the sensors or more detailed electronic models for the small cleft between the cell and transistor should be included in the coupling model.

**Keywords** Electrophysiology · Extracellular recording · Neurons · Patch clamp · Voltage clamp

### Introduction

The electrical coupling of neuronal cells to metal microelectrodes and non-metallized field-effect transistor (FET) gates has been the subject of intense study in recent years. There are many different applications where the extracellular signal recording offers a new, very promising characterization tool, especially for environmental monitoring and in pharmacological and neurological studies. The biosensor research aims to produce a sensory system by combining biological and electronic converter elements. The concept of a whole-cell sensor, which uses the cellular/microelectronic interface for the detection of drug responses on living cells, was proposed many years ago (Parce et al. 1989). Recently, portable sensor systems for the use outside of the laboratory have been developed and tested (DeBusschere and Kovacs 2001; Pancrazio et al. 2003). The fabrication and first measurements with a highly integrated CMOS biosensor array with 128×128 sensor spots on a single chip have been reported (Eversmann et al. 2003). An overview on cell-based biosensors can

---

S. Ingebrandt (✉) · C.-K. Yeung · M. Krause · A. Offenhäusser  
Max Planck Institute for Polymer Research,  
55128 Mainz, Germany

*Present address:* S. Ingebrandt  
Institute for Thin Films and Interfaces (ISG2),  
Forschungszentrum Jülich, 52425 Jülich, Germany

*Present address:* A. Offenhäusser  
Thin Films and Interfaces (ISG2), Forschungszentrum Jülich,  
52425 Jülich, Germany

*Present address:* C.-K. Yeung  
Department of Chemical Engineering,  
University of Science and Technology,  
Clear Water Bay, Kowloon, Hong Kong

*Present address:* M. Krause  
Robert Bosch GmbH, Wernerstrasse 51, 70469  
Stuttgart-Feuerbach, Germany

be found in Pancrazio et al. (1999). Additional to these applications, the hybrid sensors offer a non-invasive means in electrophysiology. For real use in electrophysiology the ion-current contributions to the total extracellular signal shapes need to be clarified. Future projects aim to create spatially controlled two-dimensional neuronal networks on extracellular devices to investigate the physiological development of these cultures in vitro.

Despite all these activities for the design and fabrication of very potent amplifier systems, the electrical coupling of a single cell to a single sensor spot and the theoretical description of this contact are still under discussion. The explanation of the extracellular recorded signal shapes was first attempted using an equivalent electrical circuit, the point contact model, which describes the cell sensor contact (Regehr et al. 1989). The coupling of large invertebrate neurons with FET sensors was described using the equivalent circuit models and distributed systems as given by the two-dimensional cable theory (Fromherz et al. 1991; Jenkner and Fromherz 1997; Weis and Fromherz 1997). The point contact model later took the contribution of voltage-gated ion-channels in the contact region between the cell and transistor into consideration (Fromherz 1999). All xdescribed signals in these works were an averaged recording over a number of sweeps in order to overcome the noise levels of the devices and recording systems. In this article we report individual extracellular signals from single mammalian neurons, which were directly located on top of single transistor gates, recorded without any signal averaging and without any active filtering. Interpretation of the signal shapes was done by individually simulating the extracellular recorded signals in PSpice (OrCAD PSpice 9.1, OrCAD Inc., ©1986–1999). For the cell–transistor coupling measurements we use the whole-cell patch-clamp technique (Hamill et al. 1981). In the voltage-clamp mode it is possible to control the activity of the voltage-gated potassium ion channels. Once a neuron is attached to a transistor gate, the inherent potassium currents can be monitored by the patch-clamp pipette and the FET simultaneously.

As a cellular system, we have chosen single neurons of explant brain-stem slice cultures from embryonic Sprague-Dawley rats (E15–E18). After adherence of slices to the laminin-pretreated sensor surfaces, neurons tend to migrate from the slice onto the sensor surface. This characteristic of explant slice cultures has already been used for the design of very precise and stable neuronal grid patterns (Yeung et al. 2001). However, the migration of the neurons on the surfaces tends to be a disadvantage for our measurements, because the cell–transistor contact is rather unstable over an extended period of time. Once a cell is attached to one of the gates of our sensor chip, the cell–transistor coupling measurements are started. The randomly migrated neurons have higher transmembrane ion currents compared to dissociated cultures (Ingebrandt 2001) or brain slice neurons on grid patterns (Lauer et al. 2002).

## Materials and methods

### Sensor chips

The p-channel FET devices used for cell–transistor coupling measurements in this study were first described by Offenhäusser et al. (1997). The fabrication process was further modified to lower the series resistance of the source and drain contact lanes (Krause 2000).

The transistor array consists of 16 transistor gates arranged in a 4×4 matrix in the center of a 5×5 mm<sup>2</sup> silicon chip. FET devices with gates spacing of 200 μm and gate sizes of 2×8 μm<sup>2</sup> (channel length times width) were predominantly used in the present study. The size of the gate oxide area exposed to the electrolyte was 6×8 μm<sup>2</sup> and the gate oxide thickness was 10 nm. The chips were encapsulated as previously described (Offenhäusser et al. 1997; Krause 2000) and were electronically stable for repeated use. Before cell culturing the FET devices were cleaned using cotton buds and ultrasonication for 10 min in 2% detergent (Hellmanex II, Helma, Mühlheim, Germany) to remove cell debris from previous usage. The surfaces were then further cleaned and activated by treating the cell culture containers for 30 min at 80 °C in 20% H<sub>2</sub>SO<sub>4</sub>. After rinsing with sterile water, FET surfaces were primed with 25 μg/mL of laminin reconstituted in sterile phosphate buffered solution (PBS) (Laminin 1243217, Boehringer, Germany; PBS buffer, pH 7.4, Dulbecco PBS solution, no. 14040-083, Life Technologies, Germany).

### Cell culture

Cultures of brain-stem slices were prepared as described by Yeung et al. (2001), which is a further modification of the method described by Gähwiler (1981, 1984). In short, 250-μm thick coronal sections of the brain stem of E15–E18 Sprague-Dawley rats were cut using a McIlwain tissue chopper. Coronal sections of brain-stem slices were harvested in brain slice culture medium (pH 7.4) made from HAMS F10 supplemented with 20% fetal bovine serum and 4 mM glutamine (all from Sigma). After an initial 4–5 h incubation period (37 °C, 5% CO<sub>2</sub>), slices were positioned at the edge of the laminin-primed device surface. In all FET devices, a minimal amount of culture medium was added during the initial adherence of slices. After 2–3 days in culture, slices adhered completely and the culture containers were filled with medium.

A typical culture contained different neuronal cell types, which have been characterized in previous work (Sivaramakrishnan and Oliver 2001). The voltage-gated transmembrane currents of cells from explant cultures were higher than those obtained using dissociated cultures, which were previously used in neuron–transistor coupling experiments (Vassanelli and Fromherz 1999). This could be due to slice cultures still containing the

necessary supporting cells such as glial and astroglial cells and these cells had not been isolated with the use of digestive enzymes such as trypsin. It has been shown in previous studies that the supporting cells are important for early cell migration and neuronal survival (Aldskogius and Kozlova 1998; Tacconi 1998; Hatten 1999). However, in our cell–transistor coupling experiments, the presence of the neuron-supporter cells was actually a disadvantage. After 7–8 days of culture the glial supporter cells formed a dense layer on the surface, which blocked the sensitive spots from the electrically active cell bodies (Fig. 1a). In order to confirm that the coupled signals originated only from the contact of a single cell attached to a single transistor gate not enhanced by the seal of surrounding glial cells or disturbed by additional inputs from axons or dendrites, we suppressed the mitosis of the supporter cells during cell culture. The use of the anti-mitotic agent Ara-C (1  $\mu$ M  $\beta$ -D-arabinofuranoside; Gibco) between days 4 and 5 increased the neuron-to-supporter cell ratio and resulted in a more defined neuronal network on the sensor surface (Fig. 1b). Cell–transistor experiments began when the cell body of a randomly migrated brain-stem neuron was directly located on top of a transistor gate, as shown in Fig. 1c.

### Electrophysiology

Patch-clamp pipettes were prepared using borosilicate glass capillaries with a filament (no. 1810016, Hilgenberg, Germany) pulled by a horizontal pipette puller (model P-97, Sutter Instruments, USA). For patch-clamp measurements, we used an EPC 9 double patch-clamp amplifier operated with the TIDA 4.11 software (both from HEKA, Germany). The recorded current signals in voltage-clamp mode were filtered with a 10 kHz Bessel filter by the EPC 9 amplifier. Pipettes were filled with an intracellular solution (in mM): 125 K-gluconate, 20 KCl, 10 HEPES, 5 EGTA, 2 MgCl<sub>2</sub>, 0.5 CaCl<sub>2</sub>, adjusted to pH 7.4 with KOH. The resistances of the pipettes were 3–6 M $\Omega$ . Before commencing patch-clamp measurements, the culture medium was exchanged with extracellular solution containing (in mM): 150 NaCl, 5 KCl, 2.5 CaCl<sub>2</sub>, 1 MgCl<sub>2</sub>, 10 HEPES, 10 glucose, adjusted to pH 7.4 with NaOH and incubated for 1 h.

### Measurement procedure

Voltage-clamp protocols were implemented for the initial characterization of single brain-stem neurons and for the cell–transistor coupling measurements. Cellular membranes were opened by light suction applied to the patch-clamp pipette. Only a series resistance lower than 20 M $\Omega$  was accepted for the neuron–transistor coupling measurements. Initial cell characterization was performed using the voltage-clamp protocol shown in Fig. 2. The neurons were clamped at –90 mV holding voltage. Eleven repetitive stimulation pulses starting from this holding

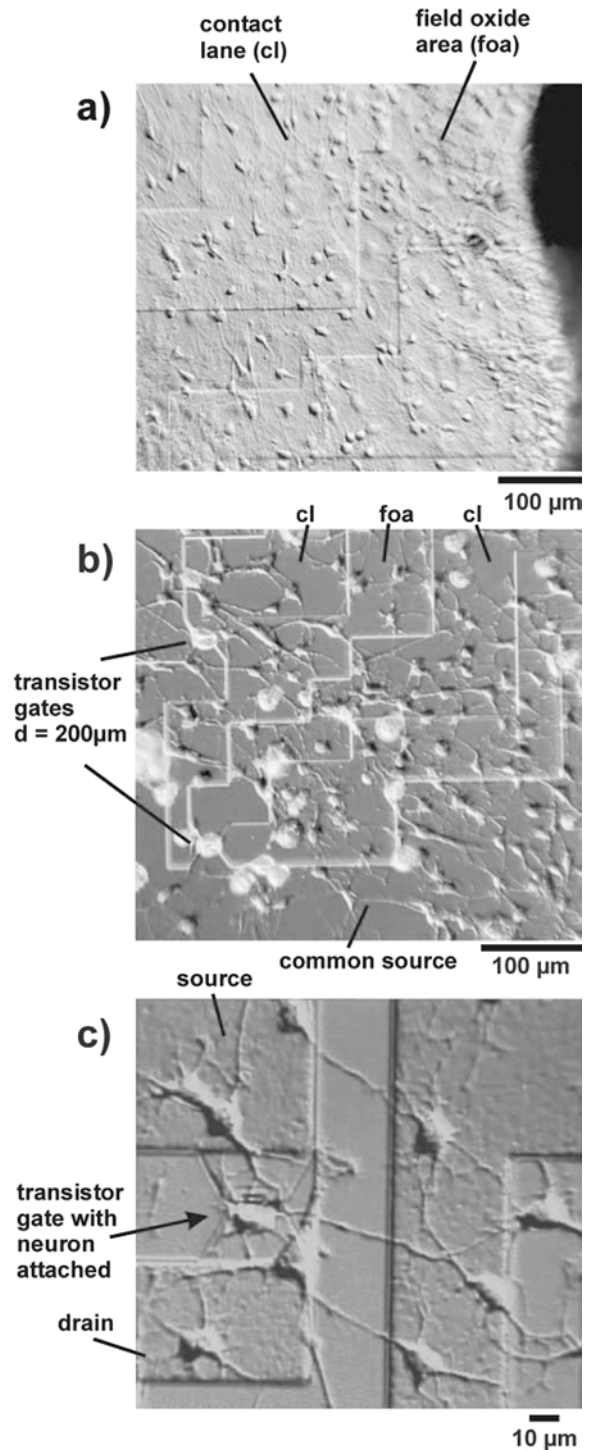


**Fig. 1a–c** DIC images of the brain-stem neuron culture on the FET surfaces. In (a) an untreated brain-stem slice culture after 6 DIV is shown. Glial cells form a dense layer for the neuronal cells. On the right-hand side the slice was cultured. If (on a different chip) the culture was treated with Ara-C, the neurons (6 DIV) form a clear network. (b) Only a few supporter cells are visible at the surface. In (c), one neuron (5 DIV, different chip) is directly located on the transistor gate and can be used in a neuron–transistor coupling measurement

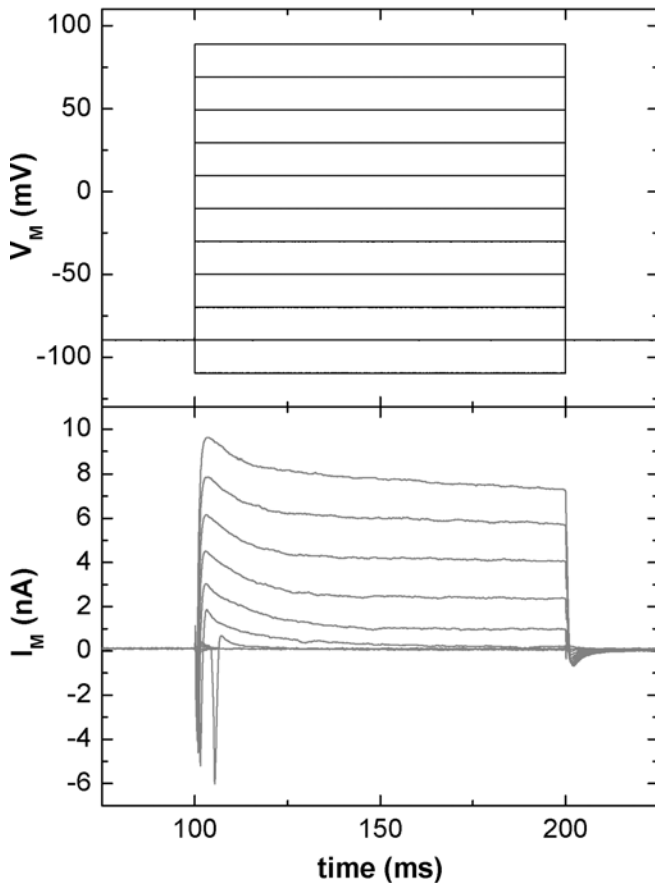


**Fig. 2** Voltage-clamp protocol for the electrophysiological characterization of the brain-stem neurons. The protocol starts with a negative pulse to  $-110$  mV (*upper trace*). The pulse steps increase up to  $+90$  mV, with a step width of  $20$  mV. In the *lower trace* the transmembrane current monitored by the patch clamp is shown

value to  $-110$  mV up to  $+90$  mV were applied. The total processing time was  $3.3$  s for this characterization experiment. This rapid data acquisition ensured that the parameters of the cell–pipette and cell–transistor contact were not significantly changed during the measurements. The brain-stem neurons in the characterization measurements (Fig. 2) showed very high voltage-gated membrane currents. In addition, a protocol for averaging a certain amount of stimulation steps was designed, using repetitive stimulation with the same step heights according to Vassanelli and Fromherz (1999). This type of experiment took much longer data acquisition time (approximately  $60$  s for averaging  $100$  sweeps in our set-up). In these cases, progressively decreasing cell viability was observed, as indicated by an increasing leak current. The averaged values of the potassium currents were then always lower than the maximum potassium current in the first stimulation pulses.

However, our rapid data acquisition represents a rather unusual electrophysiological patch-clamp protocol. In electrophysiology it is known that the slow (or type-C) potassium channels are inactivated with time constants in the order of seconds. Nevertheless, for our coupling experiment the rapid single-step protocol suited best,

because we can be sure that the electrical parameters of the cell–sensor contact did not change in this short period. For the measurements shown in this article, only such recordings were used, in which the rapid single-step characterization protocol gave sufficient signal amplitude in the transistor signal with a total process time of  $3.3$  s.

### Recording system

The FET signals were recorded using a new generation of the custom-made 16-channel amplifier previously described (Sprössler et al. 1998, 1999). These amplifiers use a feedback circuitry for offset compensation of the amplifier output, which arises from the drain-source current of the FETs at the input, to compensate for slow DC drifts of the sensor chips. The time constant of the feedback loop was in the range of seconds and the  $3$  dB point of the set-up was determined to be  $1.8$  Hz. In a control experiment, not reported here, the signal shapes of the cellular signals were found to be too rapid to be affected by this feedback loop. The high-frequency cut-off point of the amplifier system was determined using test pulses generated with a frequency generator as input signals. It was found that the transistor and the amplifier system could be sufficiently described as low pass with a time constant of  $\tau = 0.3$  ms. The recording bandwidth of our system is therefore about  $0.1$  Hz– $3$  kHz without the use of any active filtering. The low pass of the amplifier was taken into account in the signal simulation circuit (Fig. 4, right box).

The next major improvement was the use of a battery voltage supply for all electronic components of the FET amplifier system. This completely disconnected the amplifier system from the power supply, which reduced the total noise of the FET output significantly. In the present study, the output channel of the transistor gate, where the patch-clamp contacted cell was located, was connected to the external input of the EPC 9 amplifier. The whole measurement was processed by the TIDA software, which ensured quick data acquisition. All measurements were carried out with an Ag/AgCl wire as a reference electrode for the patch-clamp amplifier and for the FET device.

Cell–transistor coupling experiments were performed under an incident light differential interference contrast microscope (AxioTech Vario DIC, Zeiss, Germany) with a small diameter  $20\times$  immersion objective (UMPLFL  $20\times$ W/0.50 UIS-Obj. AA33, Olympus, Germany).

## Results

### Simulation of the neuron–transistor contact

#### Measured signals

A typical neuron–transistor coupling experiment is shown in Fig. 3. In Fig. 3a the 11 voltage stimulation

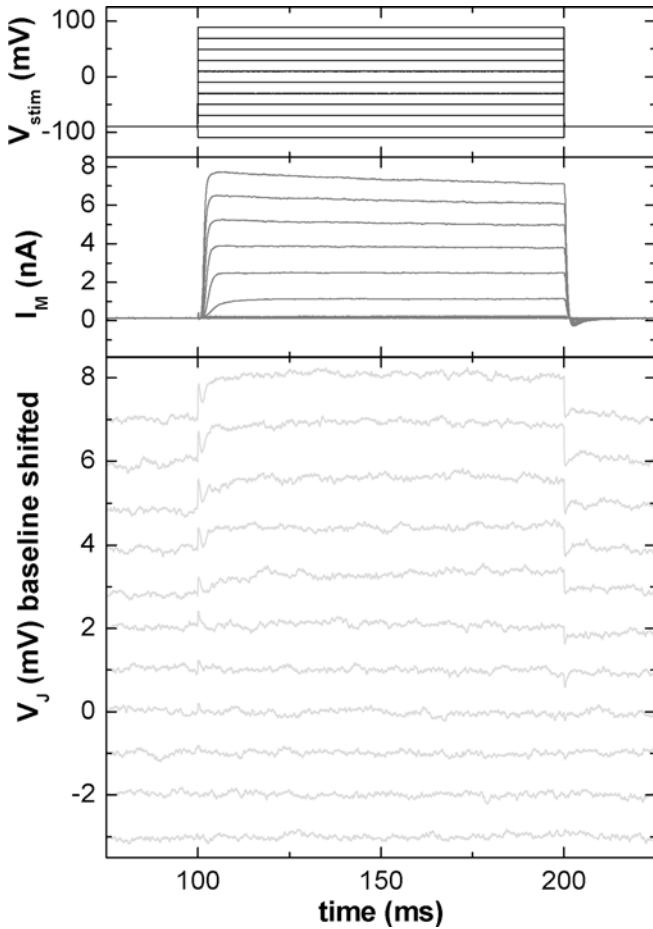


**Fig. 3** Coupling measurement using a brain-stem neuron attached to a transistor gate. The *upper trace* shows the stimulation pulses, which lead to quick capacitive peaks in the recorded FET signal. The recorded peaks and the stimulation pulse amplitudes showed a linear relation in our experiments. The *middle trace* shows the transmembrane potassium currents at each step. In the *lower trace* the un-averaged response of the FET is shown. The signal is composed of the quick initial spikes and slow components caused by potassium ion influx into the contact region

steps are shown. The patch-clamp pipette monitors higher transmembrane currents in the positive direction (Fig. 3b), which are caused by voltage-gated potassium channels in the cellular membrane. The plot in Fig. 3c shows the FET recording. In this plot the baselines of the FET signals are shifted to higher values for each step to aid better visualization. The FET signal can be clearly identified as a composite of fast capacitive and slower active ion currents. The signal contains narrow peaks at the beginning and at end of the stimulation pulse. The rectangular voltage stimulation pulses (Fig. 3a) cause a capacitive current into the contact region as quick positive peaks at the beginning and quick negative peaks at the end of the stimulation pulses. In all extracellular recordings we found a linear dependency of the capacitive peak amplitude to the amplitude of the voltage stimulation pulses. As the slower potassium currents through the cellular membrane become higher with higher stimulation steps (Fig. 3b), an increased response

of the FET signal to the potassium influx into the cleft between the cell and transistor can be seen.

### Point contact model

The electrical model for cell–transistor contact and its PSpice simulation circuit are illustrated in Fig. 4. The upper part shows a schematic of a cell–transistor coupling measurement. A simple equivalent circuit is applied to explain the extracellular recorded signal shapes (Regehr et al. 1989; Schätzthauer and Fromherz 1998; Pancrazio et al. 1999; Sprössler et al. 1999). The patch-clamp pipette (left side) attaches the cell and after compensation of all series resistive and stray capacitive components ( $R_S$ ,  $C_{Fast}$ ) the voltage  $V_M(t)$  of the cytoplasm is fully controlled by the patch-clamp amplifier. The separation of the cellular membrane and the gate results in an extended cleft of electrolyte, which is described by a specific conductance  $g_J$ , defined as the global seal conductance per junction area  $A_{JM}$ .

The membrane area of the cell is divided into the free and the attached parts with  $A_M = A_{FM} + A_{JM}$ , whereas for the respective capacitance  $C_{JM}$  and  $C_{FM}$  a typical specific membrane capacitance  $c_M = 1 \mu\text{F}/\text{cm}^2$  is used. The membrane contains various channels ( $i$ -type) with time- and voltage-dependent and independent specific ionic conductance  $g^i$  and with electrochemical driving forces  $E^i$ . In the commonly used point contact model these  $\text{Na}^+$ ,  $\text{K}^+$  and leakage currents are described by Hodgkin–Huxley elements (Hodgkin and Huxley 1952). The ion-channels in the contact region may have different opening properties or different densities. Therefore, scaling factors for each individual current part are introduced in the model, indicated by  $g_{JM}^i = X^i g^i$  with  $X^i$  as scaling factors. It is assumed that for all current parts the same conductance  $g_J$  in the cleft between the cell and transistor is valid. The specific capacitance of the gate oxide is  $c_{JG}$ . Kirchhoff's law determines the extracellular voltage  $V_J(t)$  with the current through the attached membrane, through the gate oxide and along the seal (Fig. 4, upper part):

$$c_{JG} \frac{dV_J(t)}{dt} + g_J V_J(t) = c_M \frac{d(V_M(t) - V_J(t))}{dt} + \sum_i g_{JM}^i (V_M(t) - V_J(t) - E_{J0}^i) \quad (1)$$

Three approximations are made:

1. The capacitive current  $c_{JG} dV_J(t)/dt$  through the gate oxide can be neglected.
2. The potential at the point contact  $V_J(t)$  is small compared to the membrane voltage, with  $V_M(t) - V_J(t) \approx V_M(t)$  or  $V_J(t) \ll V_M(t)$ .
3. It can be assumed that the ion concentrations in the cleft do not change with respect to the bulk electrolyte, implying unchanged reversal voltages  $E_0^i$  and thus unchanged gating properties of the potassium channels.

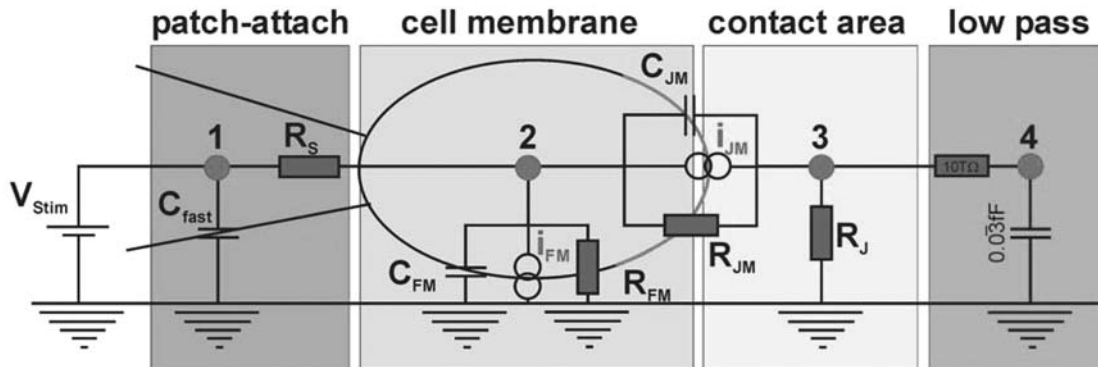
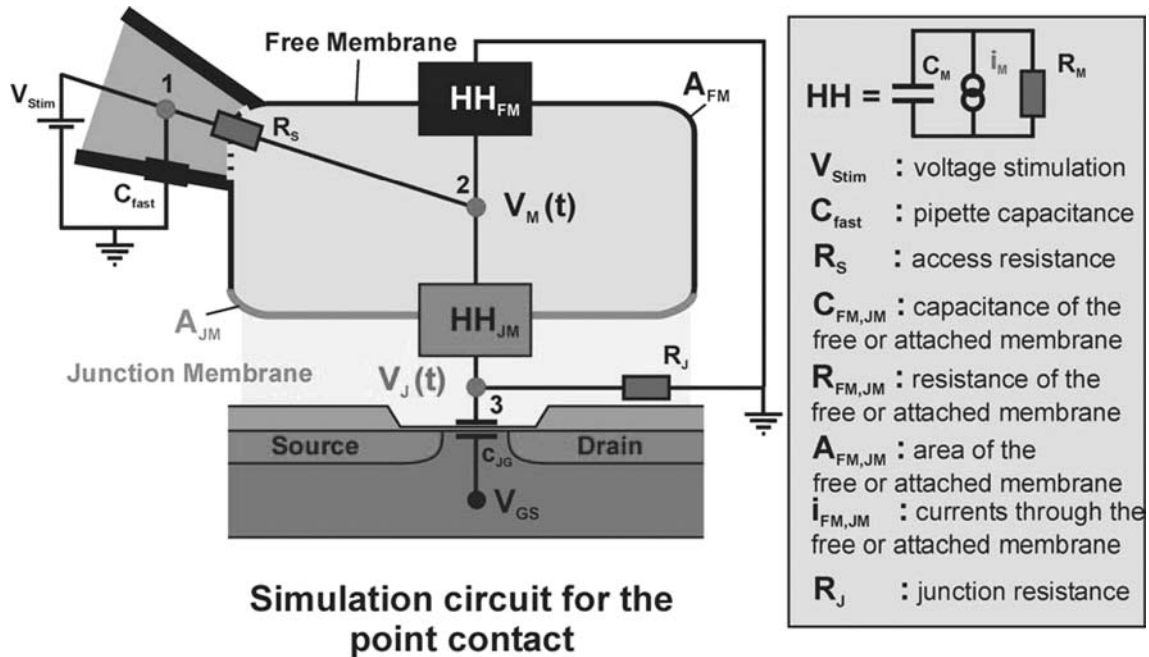


**Fig. 4** Schematics of a cell–transistor contact (*upper left*). The cell is directly located at the transistor gate and attached by a patch-clamp pipette from the left side. The cellular membrane has been divided into attached and free membrane parts. In the point contact model, Hodgkin–Huxley elements usually take the contribution of the voltage-gated ion channels into account. We are using for our signal simulation partly fixed values from the patch-clamp recording ( $C_{FM}$ ,  $C_{JM}$ ,  $R_{FM}$ ,  $R_{JM}$ ) and partly active elements ( $V_{stim}$ ,  $i_{FM}$ ,  $i_{JM}$ ) as input into the PSpice circuit. The “Hodgkin–Huxley-like” elements (HH) composed of a resistor, a capacitor and an active current source are given in the legend on the right side of the figure. For signal simulation the point contact model has been implemented in PSpice (*lower part*). On the *right-hand side* of the PSpice circuit the FET/amplifier electronics can be sufficiently described by a low pass with a time constant of  $\tau = 0.3$  ms

The third approximation is not as straightforward as the first two. Here a short assumption using simplified geometry can help. We assume the attached membrane area as a disk with 100 nm distance from the surface and 10  $\mu\text{m}$  cell radius. With this, a volume of 31 fL in the cleft is calculated. With an extracellular potassium concentration of 5 mM, this leads to a total number of about  $9 \times 10^7$  potassium ions in the cleft. We measure a whole-cell potassium current of 10 nA, from which 10% are transferred through the cleft, which has a seal

resistance of 1 M $\Omega$ , resulting from our simulations. This leads to a voltage signal of 1 mV (compare, for example, Fig. 3, highest pulse), which corresponds to the amplitudes of our recordings. A potassium current of 1 nA in 100 ms is carried by a total number of  $6 \times 10^8$  ions flowing along the cleft during the stimulation pulse. We assume now, in a “worst case scenario”, that all potassium ions are trapped in the small volume and that no diffusion takes place out of this area. This assumption will highly overestimate the accumulation of potassium under the cell, because the quick relaxation of the FET signal suggests a strong diffusion of potassium ions in a millisecond time scale.

Even with this estimation of an accumulation effect in a closed volume, we obtain an increase of potassium concentration of 5 mM to just 37 mM in the cleft. By taking diffusion into account, the real situation will be at a concentration between these values, which will just have just a minor influence on the gating of the ion channels. In addition, such a gating would lead to smaller ion-currents into the cleft and can therefore not be accounted for by the larger signal amplitudes measured by the FET.

By including the three above approximations into Eq. (1), we obtain:

$$V_J(t) = \frac{1}{g_J} \left( c_M \frac{dV_M(t)}{dt} + \sum_i X^i g^i (V_M(t) - E_0^i) \right) \quad (2)$$

Assuming proper compensation of the parasitic parameters, the whole-cell current density  $i_M(t)$  is described by:

$$i_M(t) = \sum_i i_M^i(t) = \sum_i g^i (V_M(t) - E_0^i) \quad (3)$$

Therefore, Eq. (2) can be written as:

$$V_J(t) = \frac{1}{g_J} \left( c_M \frac{dV_M(t)}{dt} + \sum_i X^i i_M^i(t) \right) \quad (4)$$

A simultaneous measurement of  $V_J(t)$  and  $i_M(t)$  with known specific seal conductance  $g_J$  allows determination of the differences between the conductance of the average cellular membrane and the attached cellular membrane, represented by the scaling factor  $X^i$ . The specific seal conductance  $g_J$  is assumed to be equal for all current types in this model. This general specific seal conductance  $g_J$  can be measured by frequency-dependent impedance analysis (Fromherz et al. 1993). We have derived  $g_J$  from the capacitive responses in the FET signals, which are proportional in amplitude to the voltage stimulation pulses of the patch-clamp pipette. In a voltage-clamp measurement the voltage stimulation pulse is filtered by a low pass formed by the access resistance of the pipette-cell contact  $R_S$  and the compensated capacitance of the cellular membrane  $C_{Slow}$  (Sakmann and Neher 1995). The time constant  $\tau_{cell} = R_S C_{Slow}$  reduces the steepness of the stimulation pulse inside the cell by an exponential law. This predicts the resulting capacitive peaks at the contact point between the cell and transistor. The first peak is in a positive direction and the second peak in a negative direction. For the extracellular recorded amplitudes of the capacitive peaks the low-pass characteristics of the amplifier unit have to be taken into account. The final

shape and amplitude can be fitted precisely by the PSpice program.

### Simulation circuit in PSpice

The point contact model was implemented in PSpice to simulate the measurement shown in Fig. 3. All static parameters, such as resistors and capacitors for a particular measurement, can be calculated from values provided by the patch-clamp amplifier. In Table 1 are summarized the input data and basic equations of how they can be calculated. In the scheme of the simulation circuit in Fig. 4 (left box), the pipette to cell contact with the access resistor  $R_S$  and the stray capacitance  $C_{Fast}$  are shown (node 1 to node 2). The electrolyte bath is connected to ground (lower contact, node 0), which is further connected to ground contacts of the FET and the amplifier. The cellular membrane is divided into free ( $C_{FM}$ ,  $R_{FM}$ ) and attached parts ( $C_{JM}$ ,  $R_{JM}$ ). A seal resistor  $R_J$  from point contact (node 3) to the electrolyte bath describes the contact area between the cell and transistor. We characterized in a series of test pulses the FET and the amplifier system with respect to their transfer function. It has been confirmed in these experiments that a low-pass build-out of a 10 T $\Omega$  resistor and a 0.03 fF capacitor is sufficient to model the transfer characteristics of the amplifier cascade (Fig. 4, right box). PSpice offers the possibility to generate voltage and current sources from a list of data to aid input of active components into the model circuit. The traces for the voltage stimulation pulse and for the current response of the cell measured by the patch-clamp amplifier were exported from TIDA and converted into appropriate lists. The stimulation pulse was fed as a voltage source at the left side between node 1 and the ground contact. The different values for the resistors and capacitors in the simulation circuit can be derived as described in Table 1. Almost all values can be taken directly or after simple conversion from the patch-clamp measurement. It has to be noted that for a parallel circuit it is:  $C_{Slow} = C_{FM} + C_{JM}$  and  $1/R_M = 1/R_{FM} + 1/R_{JM}$ . The input into the PSpice circuit is done by the

**Table 1** Input values and their sources for the simulation circuit in PSpice. For some values, simple conversions needed to be done. The attachment factor  $\alpha$  is scaling the amount of attached and free membrane parts. By adjusting the value of  $R_J$ , the amplitude of the simulated signal is fitted. The numbering in the PSpice circuit is shown in the right column

Input value	Source	Conversion	PSpice input
$C_{fast}$	$C_{fast}$ , patch clamp	Directly	C1 1 0
$V_{stim}$	$V_{in}$ , patch clamp	Voltage source as listed in PSpice	V1 1 0
$R_S$	$R_S$ , patch clamp	Directly	R1 1 2
$C_{FM}$	$C_{Slow}$ , patch clamp	$C_{FM} = (1-\alpha) \times C_{Slow}$	C2 2 0
$I_{FM}$	$I_{Out}$ , patch clamp	$I_{FM} = (1-\alpha) \times I_{Out}$	I1 2 0
$R_{FM}$	$R_M$ , patch clamp	Current source as listed in PSpice $R_{FM} = (1-\alpha) \times R_M$	R2 2 0
$C_{JM}$	$C_{Slow}$ , patch clamp	$C_{JM} = \alpha \times C_{Slow}$	C3 2 3
$I_{JM}$	$I_{Out}$ , patch clamp	$I_{JM} = \alpha \times I_{Out}$	I2 2 3
$R_{JM}$	$R_M$ , patch clamp	Current source as listed in PSpice $R_{JM} = \alpha \times R_M$	R3 2 3
$R_J$	$R_J$ , fit value	-	R4 3 0
$R_{lowpass}$	Reference measurement	10 T $\Omega$	R5 3 4
$C_{lowpass}$	Reference measurement	0.03 fF	C4 4 0

nomenclature at the right side of Table 1 (i.e. C3 2 3 means capacitor number 3 from node 2 to node 3). For simulation of the extracellular signals, one has to keep in mind that the  $C_{\text{Slow}}$  value of the patch-clamp contact reflects the total capacitance of the cellular membrane only if the leak conductance value  $G_L$ , indicating the leak current of the pipette-attached cell, is low. Details about the compensation, amplification and cancellation circuits of the EPC 9 and the methods of high-resolution whole-cell voltage-clamp patches can be found elsewhere (Sakmann and Neher 1995; Sigworth 1995; Sigworth et al. 1995). After adjusting the amplitude of the simulated signal trace for the first capacitive peak in the FET recording by fitting the  $R_J$  value, the simulated voltage trace at the amplifier output at node 4 can be compared to the FET recordings. In Fig. 5 the simulation of the highest signal from Fig. 3 is shown in detail. The voltages V1–V4 are taken from the PSpice simulation. On the left two graphs the coupling of the voltage stimulation pulse without any active potassium current input is shown. Here the evolution of the stimulation artifacts through the circuit from node 1 to the FET recording at node 4 can be seen. If the potassium currents through the free and through the attached area parts are taken into account (right two graphs), the signal shapes of the FET recordings can be simulated.

It has to be noted that for each individual measurement the respective resistor and capacitor values from the patch-clamp measurement and the current and voltage traces need to be inserted into the circuit. We are not modeling the Hodgkin–Huxley elements and their differential equations in this simple circuit. The Hodg-

kin–Huxley-like elements in the circuit consist of a resistor, a capacitor and a real current source, which are all input data from the patch-clamp measurements.

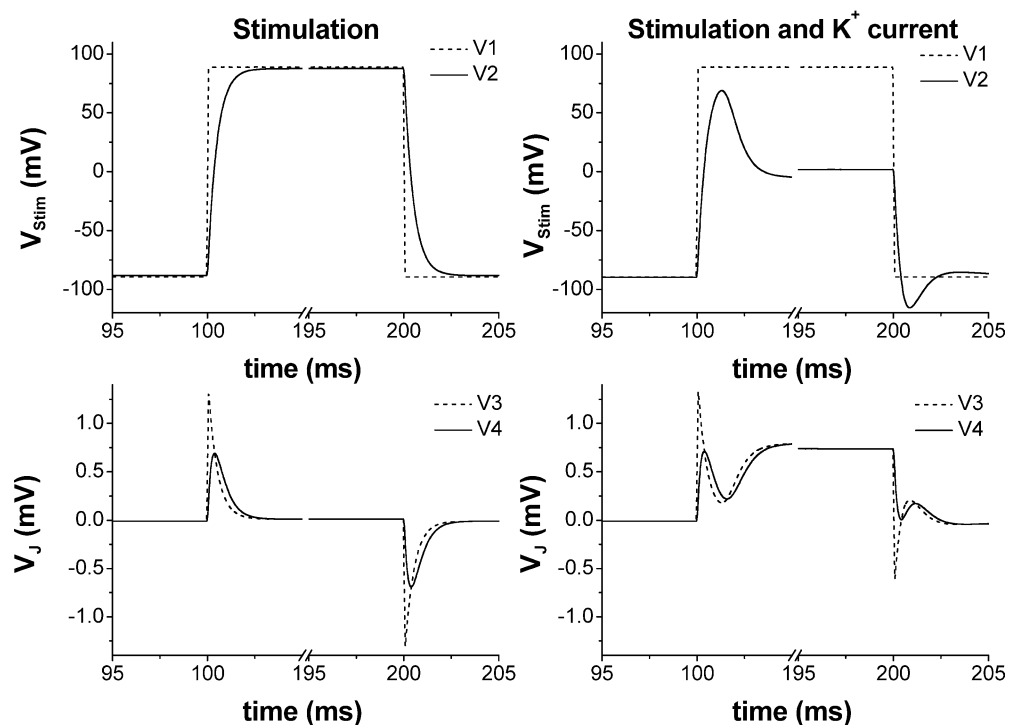
### Scaling the attached membrane part

We tested the simulated signal traces for different values of the attachment factor  $\alpha=0.1\text{--}0.5$ , which is equivalent to 10–50% attached membrane area. We found that the quick initial spike caused by the stimulation pulse remains unchanged in all cases. The differences for the slower signal part reflecting the potassium current in the contact region were found to be below 1% in amplitude. To a good approximation, the resulting signal shape and amplitude can be treated as independent from the amount of attached membrane area. The reason for this is that the values  $R_{\text{FM}}$ ,  $R_{\text{JM}}$ ,  $C_{\text{FM}}$ ,  $C_{\text{JM}}$ ,  $I_{\text{FM}}$  and  $I_{\text{JM}}$  are all scaled with the same attachment factor  $\alpha$ , which cancels out the scaling effect. For all the following simulated signals, a 10% attached membrane area was used, in accord with Vassanelli and Fromherz (1999).

### Simulated signals

The simulated signal shapes together with the original un-averaged FET recordings are shown in Fig. 6. The initial peaks in the upper graph show that the capacitive currents are well fitted. The cell was cultured for 11 days on a laminin-coated p-channel FET and was directly located on top of a transistor gate during the measurement. The resting potential of the neuron was

**Fig. 5** Simulation results for the highest recording in Fig. 3 at the four different nodes in the simulation circuit (V1–V4). On the *left side* the passive coupling of the voltage stimulation pulse is shown. If the potassium current through the free and the attached membrane parts is taken into account, the signal shape of the FET recording can be well fitted (*right side*)



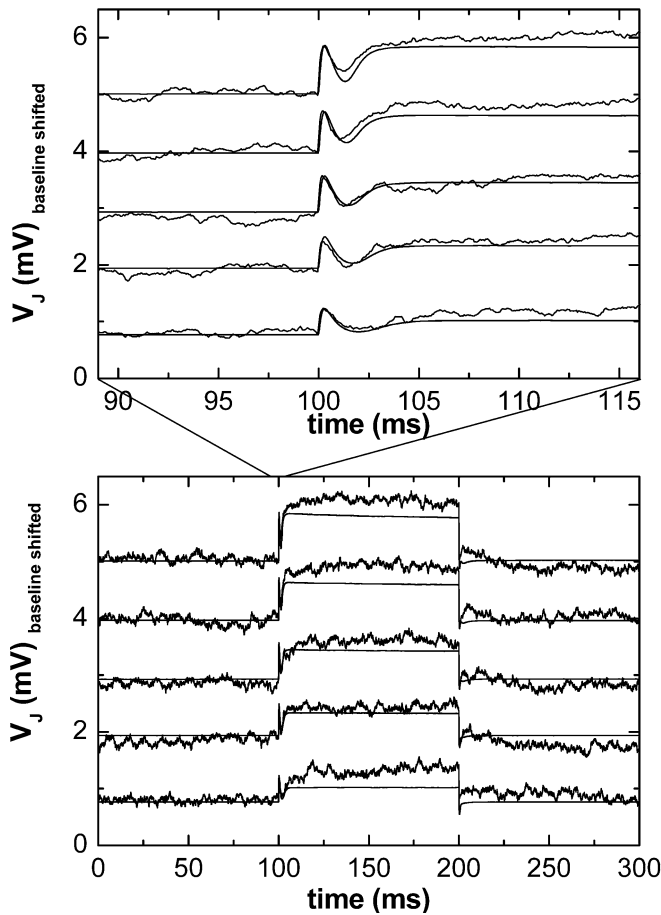


**Fig. 6** Simulation results for five different stimulation pulses. The amplitude of the simulated signal is adjusted to the quick initial peak by varying the value  $R_J$  for a single trace. For each other step the resistor  $R_J$  does not need to be changed to match the signal shapes. The *upper graph* shows that the initial peaks of the FET response are well fitted. The amplitude of the slower potassium recording remains underestimated (values at 200 ms)

–52 mV before and after the coupling measurement. The values for the patch-clamp contact ( $C_{\text{Fast}} = 7.1$  pF and  $C_{\text{Slow}} = 39.5$  pF) indicate a large neuron. The membrane resistance was  $R_M = 0.86$  G $\Omega$  and a low series resistance value of  $R_S = 12.2$  M $\Omega$  proved a good pipette–cell contact. The fitted junction resistor was  $R_J = 1.02$  M $\Omega$  for all seven steps of this particular measurement. This leads to a specific conductance of  $g_J = 0.26$  S/cm $^2$  in the cleft between the cell and transistor, which is much lower than the values reported by Vassanelli and Fromherz (1999) (0.6–1.7 S/cm $^2$ ). The low seal conductance indicates a very close attachment of the brain-stem neuron to the transistor gate. A total of eight brain stem-neurons, that were tightly attached to the gates with seal conductances ranging from 0.26 up to 0.85 S/cm $^2$ , were recorded in a similar quality. In the lower traces of Fig. 6 it can be seen that the simulation underestimates the amplitudes of the total potassium signal at the end of the stimulation pulse in all cases.

### Potassium conductances of attached and free membrane parts

In Fig. 7 the specific ion-conductances obtained with the patch-clamp amplifier and the FET responses are compared. The FET overestimates the membrane conductance for all values. This was observed in previous work (Vassanelli and Fromherz 1999; Straub et al. 2001) and was interpreted as ion-channel accumulation in the attached membrane and hence an increased ion-current in the cleft between the cell and transistor. The difference between the patch-clamp and the FET data increases with higher ion-currents (Fig. 7), which can be compensated by a constant scaling value of  $X = 1.5 \pm 0.2$ . With the maximum specific membrane conductance of the cellular membrane for potassium ions  $g_M$  of 1.6 mS/cm $^2$ , a maximum total conductance  $G_M$  of  $6.16 \times 10^{-8}$  S can be calculated using the total membrane area. With a conductance of 20 pS per channel (Storm 1990; Bossu and Gähwiler 1996), a total of about 3080 channels are active in the whole cellular membrane. The accumulation of the potassium current in the attached membrane area implies that approximately 150 ion channels (i.e. 50% more than the average value) should be additionally trapped in the junction area. However, the effect could also be explained by assuming a 1.5 times larger resistance for the specific potassium current in the cleft compared to the capacitive current.

### Discussion

In this study the neuron–transistor coupling properties of brain-stem neurons attached to extracellular FETs

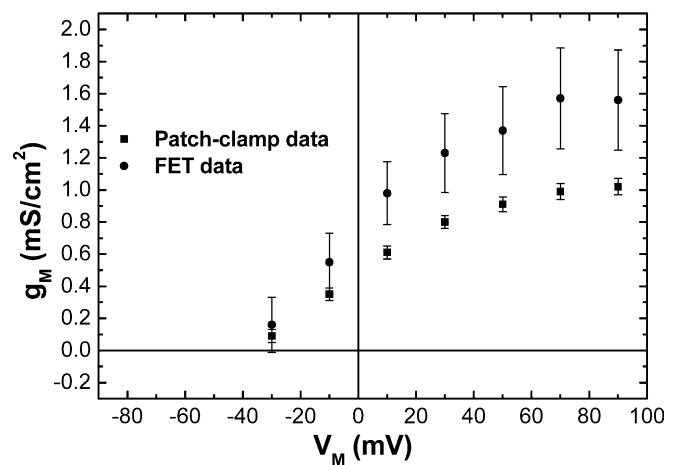


**Fig. 7** The FET signal at the end of the stimulation pulses shows higher amplitude compared to the capacitive peaks. This can be caused by accumulation of ion-channels in the contact region, higher activity of the ion-channels in this region or different conductivity for different ion-current types in the cleft between the cell and the surface. The transistor (*upper values*) overestimates the potassium current responses of the patch-clamp amplifier (*lower values*) by a factor of  $1.5 \pm 0.2$ . The error bars were calculated from the noise levels of the signals

were investigated. We used single neurons from organotypic brain-stem slices for our experiments. After 4–6 days of culturing, the neurons tend to migrate onto the laminin-primed sensor surfaces. The neurons formed tight contacts to the single transistor gates. In this study we focused on voltage-gated potassium currents (K-type), which were monitored with a patch-clamp pipette and a transistor simultaneously.

In agreement with other reported results from hippocampal neurons (Vassanelli and Fromherz 1999) and transfected cells from the HEK293 cell line (Straub et al. 2001), we observed an enhanced response of the transistor to the potassium currents. The classical interpretation of these effects is that either an increased number of ion-channels is present in the attached membrane area or the activity of the ion-channels in the attached region is raised compared to the free membrane. The amount of increased activity or increased number of channels should be 50% higher than in the overall membrane, which equals the lowest value reported by Vassanelli and Fromherz (1999) (accumulation factors 1.5–6). Our signal simulations suggest that the transistor response is more sensitive to the slower potassium current part of the extracellular signal compared to capacitive coupled peaks caused by the voltage stimulation pulses. This could either be caused by an additional effect like the ion sensitivity of the chip surface or by electrodiffusion processes in the small cleft, where ions become trapped in the small volume between the cell and transistor. It is obvious that the PSpice model of a simple, electronic point contact is rather too simple to fully explain the signal shapes. However, it was precise enough to mimic the signal shapes of the stimulation artifacts and – in tendency – the shape of the slow potassium responses. Another suggestion for the additional effects might be that the prerequisite in the point contact model, that the resistor  $R_j$  in the cleft is the same for all types of current (capacitive current transferred by displacement of all ions compared to a current just carried by potassium ions), is not completely correct.

The use of extracellular sensors in electrophysiology still has some drawbacks. It is obvious that the close adhesion of the neurons on the sensor spots is affecting the recorded signal shapes. When the system is used to monitor ion-currents, only qualitative observations can be made with the presently used models. If cells are randomly spreading onto the sensor arrays, they have only a very low probability of establishing contact with the sensitive spots. In explant cultures, the cellular network is highly dynamic in terms of migration and the neuron–transistor contact is only stable for a few hours. In the past there have been several approaches made to trap cells on laminin-imprinted structures (Yeung et al. 2001) and to align the laminin imprints on top of the sensor surfaces (Lauer et al. 2001) or to trap neurons inside micro-mechanically designed cages (Zeck and Fromherz 2001). All these solutions require a sophisticated technical effort. Therefore the extracellular sensors will not have the potential to fully

replace the patch-clamp measurement tool in electrophysiological research. Nonetheless, the planar chip approach offers the possibility to record from many different sensor spots at the same time. The functional coupling of cellular networks to extracellular devices offers the possibility to monitor signal propagation inside such networks and to investigate the information transfer, processing and storage procedures in neuronal tissue. This is the main advantage compared to the patch-clamp method, where only a few cellular responses can be monitored at the same time because of spatial limitations of the measurement set-ups. The extracellular sensor system offers an additional tool in neuronal and electrophysiological research. Our procedure for the simulation of individual extracellular recorded signals in PSpice described in this study appears to be precise only for the capacitive stimulation artifacts, whereas the signal amplitudes between the artifacts and the slower potassium part do not match. For a complete understanding of the signal shapes in future, the point contact model needs to be extended in terms of electrodiffusion, ion-sensitivity of the surface or different conductivity for different ionic currents in the cleft between the cell and sensor surface. With this simulation circuit, it would also be possible to model signal shapes of cell–transistor coupling measurements in current-clamp mode. Further studies will focus on the investigation of these natural signal shapes of mammalian neurons cultured on FET arrays.

**Acknowledgements** We acknowledge Prof Dr W. Knoll (Max-Planck-Institute for Polymer Research, Mainz), in whose group this project was initiated. We thank Prof Dr A. Maelicke (Johannes Gutenberg University of Mainz, Germany) and his group for the use of their animal facility, and Mr Lacher, Drs T. Zetterer and W. Staab from the Institute for Microtechnique, Mainz, for the support during fabrication of the FET sensors. We acknowledge the excellent technical support of Mr Müller and Mr Richter and the other members of the electronic laboratory, and Mr Gerstenberg and Mr Christ from the mechanical workshop of the MPI for Polymer Research. This work was funded by the Ministerium für Bildung, Wissenschaft, Forschung und Technologie (BMBF), German Ministry of Science and Technologie (project no. 0310895). We thank Dr C. Sprössler for his work in the field of extracellular recording using FET devices and for fruitful discussions during the project.

---

## References

- Aldskogius H, Kozlova EN (1998) Central neuron–glial and glial–glial interactions following axon injury. *Prog Neurobiol* 55:1–26
- Bossu JL, Gähwiler BH (1996) Distinct modes of channel gating underlie inactivation of somatic  $K^+$  current in rat hippocampal pyramidal cells in vitro. *J Physiol (London)* 495:383–397
- DeBusschere BD, Kovacs GT (2001) A portable cell-based biosensor system using integrated CMOS cell-cartridges. *Biosens Bioelectron* 16:543–556
- Eversmann B, Jenkner M, Hofmann F, Paulus C, Brederlow R, Holzapfl B, Fromherz P, Merz M, Brenner M, Schreiter M, Gabl R, Plehnert K, Steinhäuser M, Eckstein G, Schmitt-Landsiedel D, Thewes R (2003) A 128×128 CMOS biosensor array for extracellular recording of neural activity. *IEEE J Solid State Circuit* 38:2306–2317

- Fromherz P (1999) Extracellular recording with transistors and the distribution of ionic conductances in a cell membrane. *Eur Biophys J* 28:254–258
- Fromherz P, Offenhäusser A, Vetter T, Weis R (1991) A neuron-silicon junction – a retzius cell of the leech on an insulated-gate field-effect transistor. *Science* 252:1290–1293
- Fromherz P, Müller CO, Weis R (1993) Neuron transistor – electrical transfer-function measured by the patch-clamp technique. *Phys Rev Lett* 71:4079–4082
- Gähwiler BH (1981) Organotypic monolayer cultures of nervous tissue. *J Neurosci Methods* 4:329–342
- Gähwiler BH (1984) Slice cultures of cerebellar, hippocampal and hypothalamic tissue. *Experientia* 40:235–243
- Hamill OP, Marty A, Neher E, Sakmann B, Sigworth FJ (1981) Improved patch-clamp techniques for high-resolution current recording from cells and cell-free membrane patches. *Pflügers Arch* 391:85–100
- Hatten ME (1999) Central nervous system neuronal migration. *Annu Rev Neurosci* 22: 511–539
- Hodgkin AL, Huxley AF (1952) A quantitative description of membrane current and its application to conduction and excitation in nerve. *J Physiol (London)* 117:500–544
- Ingebrandt S (2001) Characterisation of the cell-transistor coupling. Dissertation, University of Mainz; <http://archimed.uni-mainz.de>
- Jenkner M, Fromherz P (1997) Bistability of membrane conductance in cell adhesion observed in a neuron transistor. *Phys Rev Lett* 79:4705–4708
- Krause M (2000) Untersuchungen zur Zell-Transistor Kopplung mittels der Voltage-Clamp Technik. Dissertation, University of Mainz
- Lauer L, Ingebrandt S, Scholl M, Offenhäusser A (2001) Aligned microcontact printing of biomolecules on microelectronic device surfaces. *IEEE Trans Biomed Eng* 48:838–842
- Lauer L, Vogt A, Yeung CK, Knoll W, Offenhäusser A (2002) Electrophysiological recordings of patterned rat brain stem slice neurons. *Biomaterials* 23:3123–3130
- Offenhäusser A, Sprössler C, Matsuzawa M, Knoll W (1997) Field-effect transistor array for monitoring electrical activity from mammalian neurons in culture. *Biosens Bioelectron* 12:819–826
- Pancrazio JJ, Whelan JP, Borkholder DA, Ma W, Stenger DA (1999) Development and application of cell-based biosensors. *Ann Biomed Eng* 27:697–711
- Pancrazio JJ, Gray SA, Shubin YS, Kulagina N, Cuttino DS, Shaffer KM, Eisemann K, Curran A, Zim B, Gross GW, O’Shaughnessy TJ (2003) A portable microelectrode array recording system incorporating cultured neuronal networks for neurotoxin detection. *Biosens Bioelectron* 18:1339–1347
- Parce JW, Owicki JC, Kercso KM, Sigal GB, Wada HG, Muir VC, Bousse LJ, Ross KL, Sikic BI, McConnell HM (1989) Detection of cell-affecting agents with a silicon biosensor. *Science* 246:243–247
- Regehr WG, Pine J, Cohan CS, Mischke MD, Tank DW (1989) Sealing cultured invertebrate neurons to embedded dish electrodes facilitates long-term stimulation and recording. *J Neurosci Methods* 56:91–106
- Sakmann B, Neher E (1995) Single-channel recording, 2nd edn. Plenum Press, New York
- Schätzthauer R, Fromherz P (1998) Neuron-junction with voltage-gated ionic currents. *Eur J Neurosci* 10:1956–1962
- Sigworth FJ (1995) Design of the EPC-9, a computer-controlled patch-clamp amplifier. 1. Hardware. *J Neurosci Methods* 56:195–202
- Sigworth FJ, Affolter H, Neher E (1995) Design of the EPC-9, a computer-controlled patch-clamp amplifier. 2. Software. *J Neurosci Methods* 56:203–215
- Sivaramakrishnan S, Oliver DL (2001) Distinct K currents result in physiologically distinct cell types in the inferior colliculus of the rat. *J Neurosci* 21:2861–2877
- Sprössler C, Richter D, Denyer M, Offenhäusser A (1998) Long-term recording system based on field-effect transistor arrays for monitoring electrogenic cells in culture. *Biosens Bioelectron* 13:613–618
- Sprössler C, Denyer M, Britland S, Knoll W, Offenhäusser A (1999) Electrical recordings from rat cardiac muscle cells using field-effect transistors. *Phys Rev E* 60:2171–2176
- Storm JF (1990) Potassium currents in hippocampal pyramidal cells. *Prog Brain Res* 83:161–187
- Straub B, Meyer E, Fromherz P (2001) Recombinant maxi-K channels on transistor, a prototype of iono-electronic interfacing. *Nat Biotechnol* 19:121–124
- Tacconi MT (1998) Neuronal death: Is there a role for astrocytes? *Neurochem Res* 23: 759–765
- Vassanelli S, Fromherz P (1999) Transistor probes local potassium conductances in the adhesion region of cultured rat hippocampal neurons. *J Neurosci* 19:6767–6773
- Weis R, Fromherz P (1997) Frequency dependent signal transfer in neuron transistors. *Phys Rev E* 55:877–889
- Yeung C-K, Lauer L, Offenhäusser A, Knoll W (2001) Modulation of the growth and guidance of rat brain stem neurons using patterned extracellular matrix proteins. *Neurosci Lett* 301:147–150
- Zeck G, Fromherz P (2001) Noninvasive neuroelectronic interfacing with synaptically connected snail neurons immobilized on a semiconductor chip. *Proc Natl Acad Sci USA* 98:10457–10462